OPTOELECTRONICS AND ADVANCED MATERIALS – RAPID COMMUNICATIONS Vol. 3, No. 9, September 2009, p. 851 - 859

# Chalcogenide photonic structures

M. POPESCU*, D. SAVASTRU[a], A. POPESCU[a], S. MICLOŞ[a], A. LŐRINCZI, F. SAVA, A. VELEA, L. BASCHIR[a], M. CIOBANU[a], E. MATEI, G. SOCOL[b], I. N. MIHĂILESCU[b], H. NICIU[c]
*National Institute R&D of Materials Physics, P.O. Box MG. 7, 077125, Bucharest-Magurele, Ilfov, Romania*
[a]*National Institute of Optoelectronics, INOE-2000, P.O. Box MG. 5, 077125-Bucharest-Magurele, Romania*
[b]*National Institute of Lasers, Plasmas and Radiation Physics, 077125, Bucharest-Magurele, P.O. Box. MG. 5, Romania*
[c]*National Institute of Glass S. A., Bucharest-Romania*

Chalcogenide glasses can be tailored for getting special configurations with photonic crystal properties. A review on the advances in chalcogenide glass photonics is given. Several methods to prepare two-dimensional photonic As-S glass and three-dimensional packing have been developed, and the photonic structures have been characterized. Numerical simulations have also been performed. The chalcogenide photonic structures fabricated by micro-technological procedures are described and tuned to work in the far infrared region of the electromagnetic spectrum.

(Received September 07, 2009; accepted September 15, 2009)

*Keywords*: $As_2S_3$, Chalcogenide photonic structure, Photonic crystal, Grating, Interference

## 1. Introduction

Photonic crystals are promising structures for the control of light in a photonic integrated circuit at the radiation wavelength scale. These crystals are characterized by periodicities much larger than the atomic scale periodicity of the known crystals. The required periodicity is realized in crystalline or even in glassy materials by special techniques. The two-dimensional photonic crystals consist essentially of a thin, high refractive index dielectric slab, containing a periodic lattice of air holes. Due to special configuration and contrast of the refractive indices in air and in material these configurations can possess photonic band gaps, i.e. continuous regions of electromagnetic frequencies whose propagation is forbidden within the realized structures. The nano-photonic devices use a high refractive index contrast to achieve tight optical confinement, allowing wavelength scale resonators and wave guides bends.

The development of optical devices with similar functionality to that which the transistor provides in electronics is a "holy grail" in photonics. A photonic transistor would allow the control of high-speed optical signals by light. This would simplify and lower the cost of future optical communication networks. The challenge is to fabricate devices that operate at low optical powers and at speeds of several tens of GHz.

The concept of three-dimensional (3D) photonic crystal has been introduced independently as early as 1987 by Yablonovich [1] and John [2]. Later, great efforts have been devoted to get photonic crystals operating in various light wavelength domains, including the window around 1.5 micrometers. The photonic crystals have important applications: lossless guiding [3], tightly bent 90$^o$ waveguides [4], and on-chip integration as they can combine optical waveguides, resonators [5], dispersive devices, laser and modulators [6,7].

The chalcogenide glass (e.g. $As_2S_3$) have properties very useful for the fabrication of photonic band-gap configurations: high refraction index, photosensitivity [8, 9], transparency in infrared domain (from 800 nm up to 12 micrometers wavelength) and capability to be etched by various etchants exhibiting the properties of positive or negative photo-resists [10].

In this paper we review the photonic crystal configurations achieved in a chalcogenide glass and report our results in the formation of various photonic glass configurations in the $As_2S_3$ glass, a binary chalcogenide very stable in its non-crystalline form.

## 2. Chalcogenide glass properties

Besides high refractive index of e.g. As-S glass that allows a 2D photonic band-gap, the linear absorption losses are low over a wide range of compositions. The chalcogenides have large $\chi^3$ nonlinearity ($n_2$ from 100 to 1000 times that of silica, i.e from $3\times10^{-14}$ to $3\times10^{-12}$ cm$^2$/W comparable to AlGaAs below half-band-gap and low two-photon absorption (β)). Equally important is the figure of merit (FOM). FOM = $n_2/\beta L$, which should be >1 to enable all-optical processing, and is often >5 (~12 for $As_2S_3$).

The index of refraction of $As_2S_3$ is situated in the range 2.45-2.53, sufficiently to open a photonic band gap. The position of the absorption edge is found at 530 nm wavelength leaving a broad part of the visible spectrum accessible.

Because of high refractive index the chalcogenide glasses allow light to be trapped in small waveguides or resonators. The 2D photonic structure is a configuration in which light is tightly confined in a high-Q optical

resonator to achieve a non-linear optical response. This will lead to switching at speeds limited only by the Q of the resonator, at exceptionally low power and without interference from thermal or free-carrier induced effects.

Chalcogenide glasses exhibit strong photo-structural modifications. Their photosensitivity is due to structural rearrangements induced by the absorption of light at photon energies near the electronic band-edge of the material, leading to changes in the refractive index, shift of the absorption edge (photo-darkening and photo-bleaching) and density changes (volume expansion or volume compression). These properties have been largely used in the written Bragg gratings, directly written waveguides and last but not least for post-tuning of optical components [11]. The possibility of post-trimming the properties of individual components is highly attractive, relaxing the fabrication tolerances and allowing novel devices to be more easily created. The ability to tune the cavity resonance via a photosensitive chalcogenide film applied to the photonic crystal device appears to be very promising.

Direct laser writing [12] in arsenic-sulfur based thin films of chalcogenide glasses with intense 120 fs pulses induces a local chemical phase change via two-photon absorption to $As_2S_3$. The inscribed two-dimensional photonic crystals were subsequently etched out with a wet chemical etchant. The high refraction index of the material allows the opening of a complete band gap in diamond-like crystal structures, e.g. a "wood-pile structure".

Thin chalcogenide films are good candidate for building photonic structures. In many cases the evaporation method has been used. Pulsed laser deposition (PLD), has produced exciting results in the recent past, proved to be providing growth flexibility and high quality at low costs.

Feigel et al. [13, 14] reported 3D photonic band-gap glass configuration where two or three-beam holographic laser lithography was combined with selective etching. As above-gap radiation and thus one-photon absorption was used in these experiments, the lithographic step could only be used to fabricate a single layer at a time. Consecutive layers had to be stacked on top of each other and photonic glasses with a maximum of four layers have been reported.

An efficient method for inscribing photon-gap configurations in $As_2S_3$ has been introduced by Wong et al. [15]. The films were deposited by vacuum evaporation at 385 $^oC$ in a high vacuum evaporation chamber ($p=5\times10^{-6}$ mbar) and at low deposition rate (6 nm/s). The obtained films consisted in a molecular glass with high percent of $As_4S_6$ cage molecules. A high content of cage molecules is desirable in order to maximize the photo-polymerization effect. Fast evaporation rates are detrimental because the material will be decomposed in $As_4S_4$ cages and $S_8$ rings. Such films are less effective for photo-polymerization. Local photo-exposure of the glass will transforms the molecular glass into normal polymerized $As_2S_3$ glass. Because the transformation is topotactic neither shrinking nor expansion of the written structure do occur. This is very important for the resolution of the laser inscribed structure in the glass.

In a recent paper [16] the authors have demonstrated by Raman spectroscopy that films of As-S deposited at a slow rate suffer photo-polymerization. When the deposition rate increases the films become sulfur deficient. Fast deposited films are nevertheless unstable and phase separation occurs upon light irradiation.

## 3. Photonic glass configurations

### 3.1 Etching properties of the chalcogenide glass

As a result of irradiating the chalcogenide film by light with wavelength corresponding to inter-band absorption, many of their properties are modified, in particular their optical characteristics (absorption edge, refractive index, induced dichroism), mechanical characteristics, solubility, etc. The most studied are the optical properties and solubility because these changes are the basis for using the chalcogenide as medium for optical recording and as inorganic resist. The utilization of the films as photo-resist media is related to the irreversible solubility changes. The chalcogenides are well dissolved in many inorganic and organic solvents such as alkaline or amine solutions. After exposure the solubility rate of the films is changed, and, depending on the film's composition and the type of solvent used, it is possible to get various degrees of selectivity, defined by the solubility ratio of the exposed and unexposed areas. For different solvents and films it is observed positive or negative etching, i.e. the exposed area are dissolved either more rapidly or more slowly than the unexposed areas. We used in our experimental investigations the negative etching amine solutions.

Noticeably light sensitivity of the film was observed up to 600 nm wavelength. The formation of the groove profile of the interferential structure and kinetics of the etching, using As-S based chalcogenide photoresist were investigated in [17-19].

Fig. 1 shows the kinetics of the etching of $As_2S_3$ films for different light intensities and etching times as given in [19].

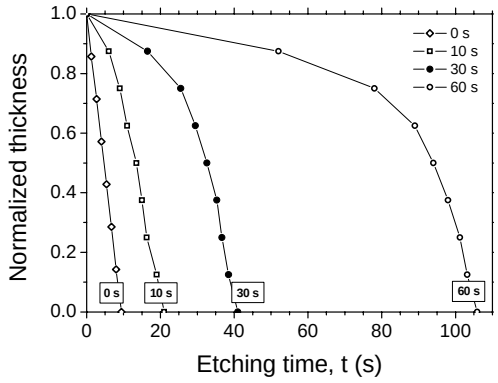


*Fig. 1. Etching curves for $As_2S_3$ chacogenide resist, for different irradiation times and amine based etchant.*

### 3.2 Photonic crystal configurated in bulk and polymer templated $As_2S_3$

Direct writing of micro-structures in a thick solid medium has proven to be a powerful method for many photonic applications [20]. Micro-explosions induced by an ultrafast femtosecond laser beam focused by a high numerical-aperture objective has facilitated the generation of micro-voids in glass [21] This has provided a method for creating 3D photonic crystal lattices with multiple-order of gaps in the near infrared wavelength region [22].

One of the directions in the fabrication of bulk photonic band-gap structures based on chalcogenides was the self-assembly of nano-spheres. This approach is elegant and simple and is suitable for mass production. Nevertheless, the flexibility of the method is very limited [23, 24]. Self-assembling of low refractive index colloidal micro-spheres has been used by Mayoral et al. [25] and Wong et al. [26] for making photonic band gaps in chalcogenides.

The fabrication and infiltration of opal-type templates by self-assembly has been demonstrated by Vlasov et al. [27].

Theoretical and experimental results of disordered photonic crystals show that the transmission properties of photonic materials are strongly affected by the disorder in the photonic structures. Recently a kind of photonic material has been obtained [28]. The material is disordered. It is constructed with a randomly oriented unit cell located on each lattice point of a periodic basic frame. Both simulation and experimental results show that the amorphous photonic material exhibits photonic gap. It seems that the formation of the photonic gap has little relation with the symmetry of the basic lattice. In contrast, the transmission properties are clearly affected by the short-range order resulting from the unit cell. Wang and Jain [29] suggest that it is possible to engineer the band-gap in amorphous photonic materials by controlling the size of the unit cell. We must mention here that recently, one-dimensional photonic crystals have been fabricated using porous silicon layers [30, 31]. The electrochemical etching was used and large photonic band gap has been obtained by tuning the etching time.

We have built two-dimensional and three-dimensional photonic crystals based on $As_2S_3$ glass starting from packing micro-spheres of diameter 280 micrometers. Fig. 2 shows the image of a 5×5 2D glass photonic configuration. High contrast of the refractive indices is achieved by using glassy spheres embedded in optical glue. Due to large sizes of the micro-spheres the photonic band gaps are in the range of microwaves. The shrinking of the lattice by careful heat treatment near glass transition temperature, determines the shift of the main photonic band gap towards lower wavelengths in the far-infrared region of the electromagnetic spectrum [32].

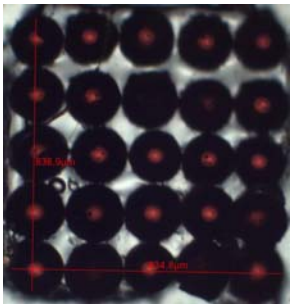

*Fig 2. 2D- photonic configuration with As-S microspheres.*

In the other experiment we have tried to use pulsed laser deposition (evaporation or flash deposition of $As_2S_3$ glass on metallic templates of very small mesh (75 micrometers) in order to achieve a distinct separation of glassy cells with the purpose to get a photonic band-gap in the far infrared region.

The metallic mesh template is shown in Fig 3.

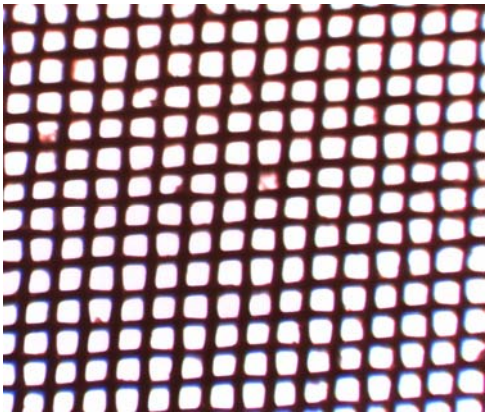

*Fig. 3. Metallic mesh with a repetition unit of ~ 75 μm.*

A larger substrate made of plastic material by melt injection, and having the mesh of 610 micrometers / 240 micrometers has been also prepared (see Fig. 4).

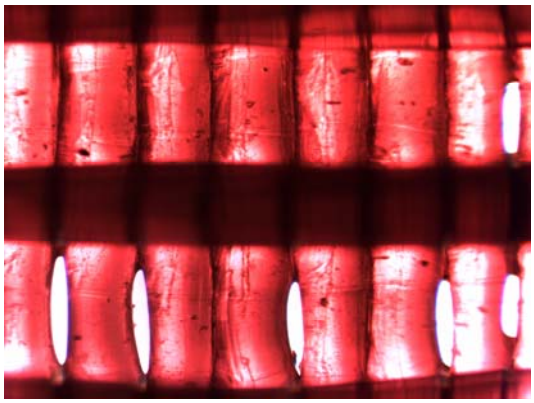

*Fig. 4. As-S grid on plastic mesh.*

The other procedure was to produce quantum dots equally spaced. Recently, Ventura et al. [33] prepared PbS quantum dots uniformly distributed in a host polymer matrix. Infrared absorption microscopy of a sample doped at a low density of 0.05 ppm shows a peak coinciding with the quantum dot absorption band at 1.4 micrometers. PbSe nano-wires grown by the template method have been prepared [34]. Nevertheless, the wires are arranged in a disordered way and more advances are necessary to ensure the equal inter-distances between the nano-wires.

To move the fundamental photonic band gaps toward the wavelengths of the telecommunication region of 1.5 μm and 1.3 μm it is necessary to have an in-plane rod spacing of the order of 1 μm and smaller. The sample area of 100 μm × 100 μm is enough large for optical spectroscopy as well as for potential devices.

We have prepared a two-dimensional arrangement of dots was obtained on glassy substrate. The PLD technique of deposition has been used. Figure 5 shows the photonic configurations. Because the configuration has a lattice constant of ~ 650 micrometers the band-gap separation could be demonstrated mainly for microwave field (THz frequencies). The studies are in progress.

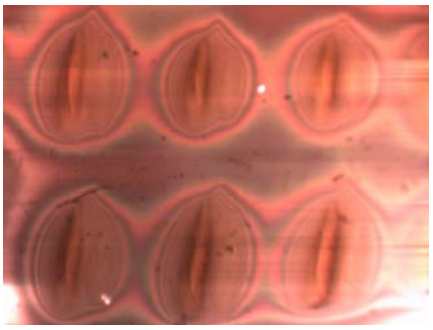

*Fig. 5. Quantum As-S dots on glass.*

## 4. Profiled holographic gratings written in $As_2S_3$ chalcogenide glass, as a first stage of a photonic glass configuration

### 4.1 Results of numerical simulations

We have performed numerical simulations with the free available numerical code MPB–MEEP developed by Joannopoulos et al. [35] at MIT, which uses the FDTD (Finite Difference Time Domain) method. We obtained the field structure after traversing the crystal configuration, as well as the width and position of the band gap. We simulated the influence of a 1-D photonic crystal on the electromagnetic radiation emitted by a source in the neighborhood. We considered the crystal made of $As_2S_3$ (n=2.45), and we considered two cases: the first one when the height of the fringes of the periodic structure is small, and secondly, when they are taller. The period of the structure was 450 nm (Figs. 6 and 7):

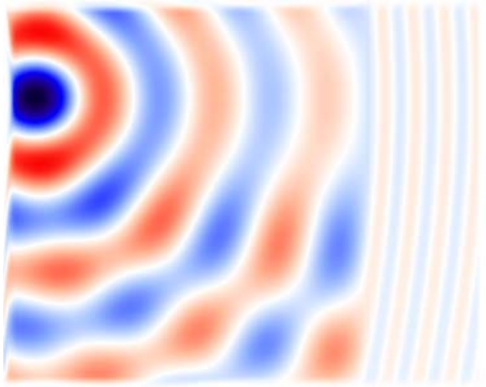

*Fig. 6. The electromagnetic field after traversing the small fringes; red = maxima; blue = minima.*

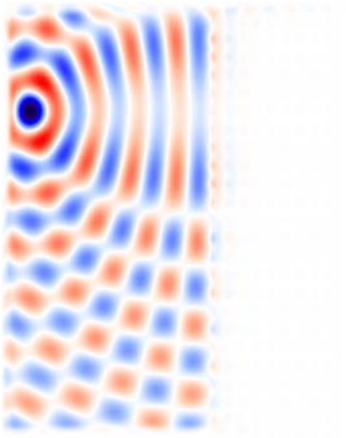

*Fig. 7. The electromagnetic field after traversing the tall fringes; red = maxima; blue = minima.*

Likewise, we determined by numerical simulations the width and the position of the band gap, for different values of the fringe, due to the fact that this value cannot be measured accurately. Results are shown in the Table 1 below.

*Table 1. Fringe width of the holographic grating as a function of the width and position of the band gap (simulation results).*

| Fringe width, r (fractions of crystal period) | Photonic band gap (Hz $\times 10^{14}$) | Photonic band gap (μm) |
|---|---|---|
| 0.2 | 6.5 – 6.8 | 0.44 – 0.46 |
| 0.25 | 2.9 – 3.1 | 0.96 – 1.03 |
| 0.3 | 2.2 – 2.7 | 1.11 – 1.36 |
| 0.35 | 2.05 – 2.3 | 1.30 – 1.46 |

We observe from the table that in order to get a band gap of approximatively 1.5 μm, the fringe must represent about 40% from the crystal's period.

### 4.2 Experimental realization and characterization of amorphous chalcogenide photonic structure

An experimental setup was achieved to record periodic structures in thin films as displayed in Fig. 4.1. An Ar-ion laser tuned on the wavelength of the optical transmission alteration was used as coherent light source. For $As_2S_3$ compounds the optimal wavelength was 514 nm. The output power of the laser beam was 500 mW. In order to obtain a coherent optical radiation a spatial filtering was done using an objective and a pinhole. Other optical components, displayed in Fig. 8, were mounted on an optical table with pneumatic dampers. Figures 9 and 10 display pictures of the experimental setup.

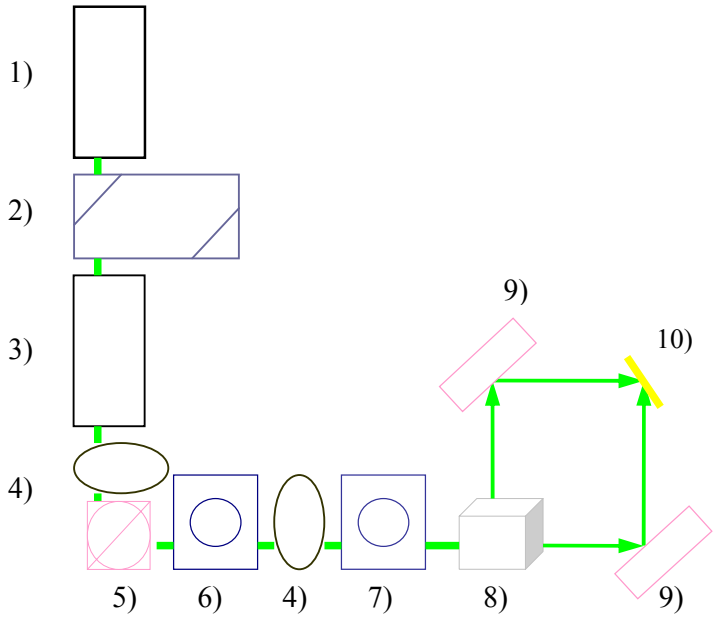


*Fig. 8. Layout of the experimental setup for holographic gratings recording in chalcogenide $As_2S_3$ thin films.*

This experimental setup is made up of the following items:

1) Ar-Ion laser, wavelength 514 nm (green)
2) Periscope – used to vertically align the laser beam
3) Telescope (beam expander)
4) Lens (focal length 100 mm)
5) Mirror – used to deflect the laser beam at 90°
6) Fourier pinhole Ø 25 μm
7) Diaphragm Ø 3 mm
8) Beam splitter
9) Mirror
10) Sample to be recorded

The exposure time to record the diffraction gratings was determined from experiments conducted according to the layout presented in Fig. 11. The diffraction efficiency was measured using a powermeter for 633 nm He-Ne laser radiation. Result to these experiments the optimal recording time was determined (Fig. 13) respecting the saturation criterion, when the intensity does not increase any more.

When the film is exposed with a power of 25 mW/arm an optimal exposure time of 5 min was obtained. The image of the $As_2S_3$ 2 μm – thick films after they were recorded using Ar laser is displayed in Fig. 12 (the darker spots represent the hidden image).

The fringe period Λ after recording was computed from the formula:

$$\Lambda = \frac{\lambda_0}{2\sin\frac{\alpha}{2}} = 0.45\ \mu\text{m},$$

where $\lambda_0 = 514$ nm , $\alpha = 70°$.

After recording and getting the hidden image these periodical interference structures were developed by etching in diethylenetriamine of 1 mol concentration. The etching time is 30 s. The film was washed in a 40 % alcohol solution. More technological specifications can be found in [36].

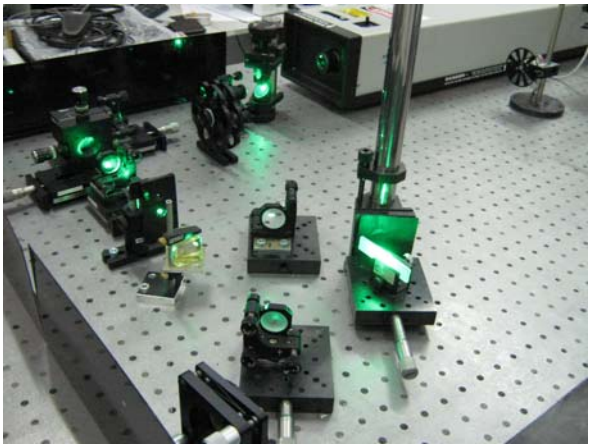

*Fig. 9. The images of the experimental setup. For Ar laser power measurements in different points of the setup was used an Energy/Powermeter GENTEC having the measuring heads PH100Si and UP12E10S-H5.*

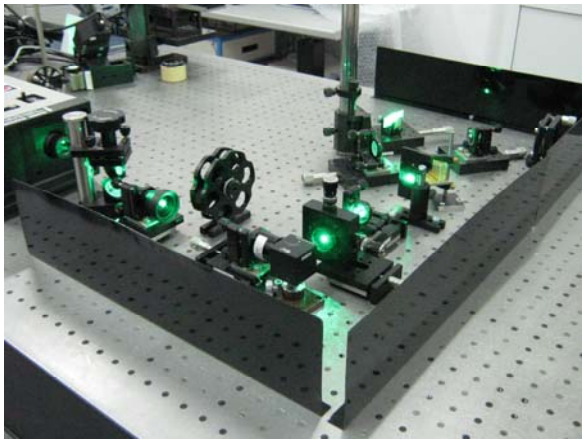

*Fig. 10. The images of the experimental setup. A 633 nm (red) HeNe laser, 12 mW power, was used to determine the transmission and diffraction intensity of the recorded samples.*

The diameter of the laser beam on each arm (distance from mirror 9 to the sample to be recorded) is 50 mm.

The film is positioned at the crossing of the beams to accomplish the recording of the diffraction pattern.

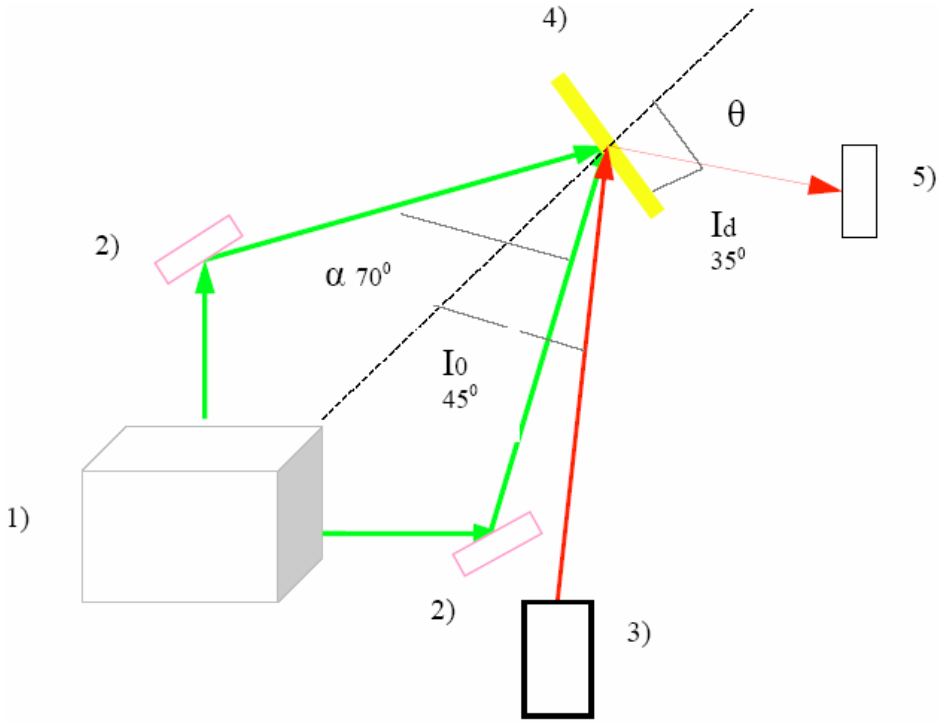


*Fig. 11. The layout of the experimental setup achieved to determine the optimal recording time of the diffraction grating: 1) Beam splitter; 2) Mirror; 3) HeNe laser (633nm red); 4) Sample; 5) Detector (GENTEC powermeter).*

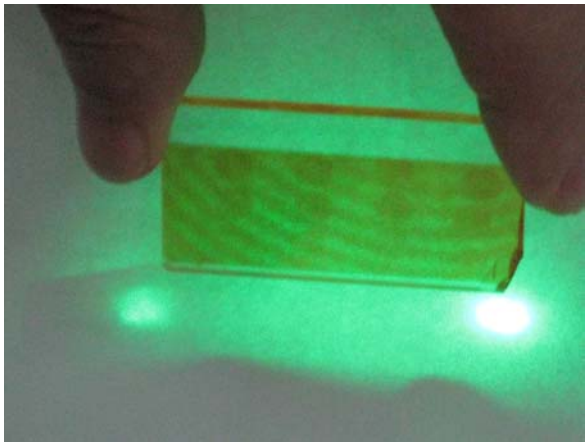

*Fig. 12. Recorded $As_2S_3$ chalcogenide film.*

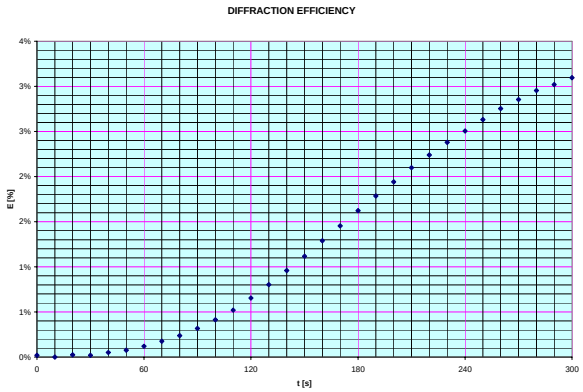


*Fig. 13. Diffraction efficiency vs. exposure time.*

After etching a periodic profile structure was obtained. The image and the light decomposition phenomenon by the profiled periodical structure after etching are presented in Fig. 14. In Fig. 15 is displayed the image of a periodic structure obtained by masking.

The incidence angle on the mirror was 45°(formed by the HeNe mirror and the normal perpendicular to the film). The diffraction angle was 35°. For measurements we used the PH100SI head and we observed that after approximatively 6 minutes of recording time T the diffraction intensity began to decrease.

*Fig. 14. Demonstration of light diffraction by the grating resulted from recording laser radiation (Ar) after developing.*

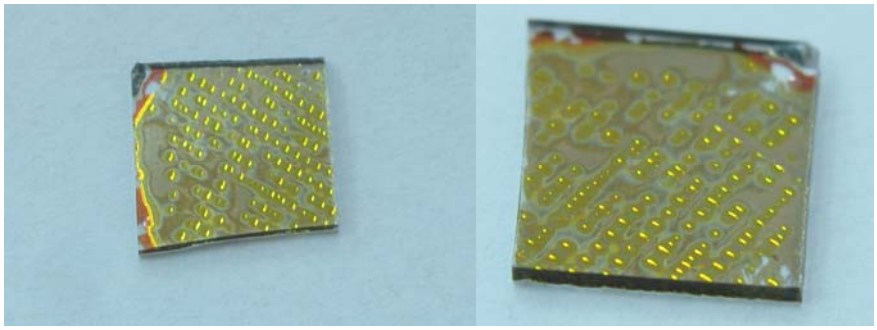

*Fig. 15. Periodic grating obtained by mask deposition.*

The thin layer (2 μm) of $As_2S_3$ was inspected using an AFM in order to observe its roughness.

The obtained image is presented in Fig. 16, remarking a maximal roughness of 11.92 nm, indicating a high quality surface.

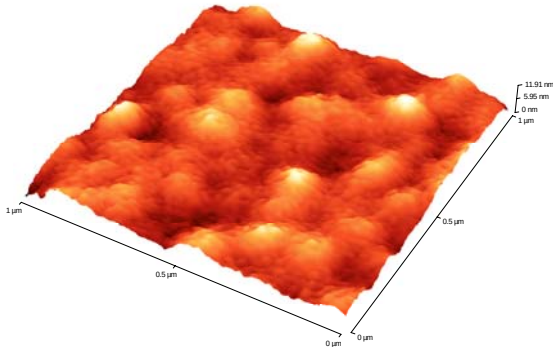

*Fig. 16. The roughness of the surface of the deposited layer.*

The hidden array, after having been obtained, was developed. As can be seen in Fig. 17, the developing process led to nanocrystaline droplets.

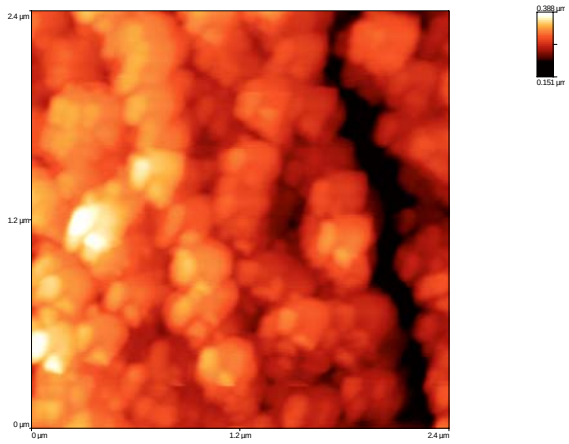

*Fig. 17. Detail of the chalcogenide developed layer.*

The obtained diffraction grating was inspected with AFM, as can be seen in Fig. 18. We can observe 11 interfringes on a distance of 5 μm, meaning a latice constant of about 450 nm (the exact pitch is 448 nm).

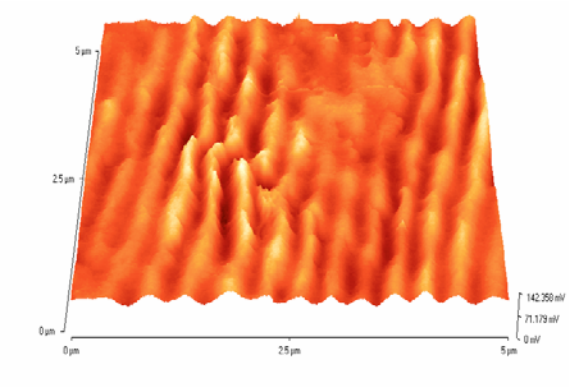

*Fig. 18. Developed diffraction grating, pitch 448 nm.*

## 4. Conclusions

Photonic crystal structures based on chalcogenide glasses have been reviewed. Various methods to get photonic band configurations were discussed.

We have built two-dimensional photonic crystals by using chalcogenide laser pulse deposition through a mask provided with holes. Etching of films illuminated by interference light allowed to prepare good gratings, to be used in the stacking of the etched glass in a wood-pile configuration. Glasses deposited or molded in the 75 micrometer mesh template, allowed to pack easily in 2D configurations, which further can be easily packed in 3D photonic crystal configurations.

## Acknowledgements

The financial support offered by the Ministry of Education, Research and Youth of Romania in the frame of the grant No. 11-073/14.09.2007 (NAFO) is kindly acknowledged.

## References

[1] E. Yablonovitch, Phys. Rev. Lett. **58**, 2059 (1987).
[2] S. John, Phys. Rev. Lett. **58**, 2486 (1987).
[3] M. Bayindir, B. Temelkuran, E. Ozbay, Phys. Rev. Lett. **84**, 2140 (2000).
[4] S. Noda, K. Tomoda, N. Yamamoto, A. Chutinan, Science **289**, 604 (2000).
[5] M. Notomi, A. Shinya, S. Mitsugi, E. Kuramochi, H-Y. Riu, Optics Express **12**(8), 1551 (2004).
[6] A. Faraon, E. Waks, D. Englund, I. Fushman, J. Vuckovic, Applied Physics Letters **90,** 07312 (2007).
[7] A. Faraon, E. Waks, D. Englund, I. Fushman, J. Vuckovic, Applied Physics Letters **90,** 213110 (2007).
[8] V. Lyubin, M. Klebanov, I. Bar, R. Rozenwaks, V. Volterra, L. Boehm, Z. Vagish, Appl. Surf. Sci. **106**, 502 (1996).
[9] V. Lyubin, T. Tada, M. Klebanov, N. N. Smirnov, A. V. Kolobov, K. Tanaka, Matter. Lett. **30**, 79 (1997).
[10] M. W. Lee, C. Grillet, C.L.C. Smith et al., Optics Express **15**(3) 1277 (2007).
[11] V. Lyubin, M. Klebanov, I. Bar, R. Rozenwaks, N. Eisenberg, M. Manevich, J. Vac. Sci. Technology, **B15**, 823 (1997).
[12] M. Deubel et al., Nature Materials **3**, 444 (2004).
[13] A. Feigel. M. Veinger, B. Sfez, A. Arsh, M. Klebanov, V. Lyubin, Appl. Phys. Lett. **83**, 4480 (2003).
[14] A. Feigel, Z. Kotler, B. Sfez, A. Arsh, M. Klebanov, V. Lyubin, Applied Phys. Lett. **77**, 3221 (2000).
[15] S. Wong, M. Deubel, F. Perez-Willard, S. John, G. A. Ozin, Adv. Mater. **18**, 265 (2006).
[16] V. I. Mikla, V. V. Mikla, Optoelectron. Adv. Mater. – Rapid Comm. **1**(6), 272 (2007).
[17] I. Z. Indutnyy, A. V. Stronski, S. A. Kostioukevich et

al., Optical Engineering **34**, 1030 (1995).
[18] I. Z. Indutnyy, M. Popescu, A. Lőrinczi, F. Sava, V. I. Min'ko, P. E. Shepelyavyi, J. Optoelectron. Adv. Mater. **10**(12), 3188 (2008).
[19] M. Popescu, F. Sava, A. Lőrinczi, A. Velea, M. Vlček, H. Jain, Philosophical Magazine Letters **89**(6), 370 (2009).
[20] H. Misawa, S. Juodkazis, 3D laser microfabrication – Principles and applications, Wiley VCH Verlag, Weinheim, 2006.
[21] E. N. Glezer, M. Miloslavljevic, L. Huang, R. J. Finlay, T. H. Herr, J. P. Kallan, E. Mazur, Opt. Lett. **21**, 2023 (1996).
[22] M. Straub, M. Ventura, M. Gu, Phys. Rev. Lett. **91**, 043901 (2003).
[23] Y. A. Vlasov, V. N. Astratov, O. Z. Karimov, A. A. Kaplyanskii, V. N. Bogomolov, Phys. Rev. **B 55**, R13357 (1997).
[24] A. van Blaaderen, R. Ruel, P. Wiltzius, Nature (London) **385**, 321 (1997).
[25] R. Mayoral, JU. Requene, J. S. Moya, C. Lopez, A. Cintas, H. Miguez, H. Meseguer, L. Vazquez, MK. Holgado, A. Blanco, Adv. Mater. **9**, 257 (1997).
[26] S. Wong, V. Kitaev, G. A. Ozin, J. Am. Chem. Soc. **125**, 15589 (2003).
[27] Y. A. Vlasov, X.-Z. Bo, J. C. Sturm, D. J. Norris, Nature **414**, 289 (2001).
[28] C. J. Jin, X. D. Meng, B. Y. Cheng, Z. L. Li, D. Z. Zhang, Phys. Rev. **B 63**, 195107 (2001).
[29] Y. Wang, S. Jian, Physics Lett. **A 352**, 550 (2006).
[30] R. S. Dubey, L. S. Patil, J. P. Bange, D. K. Gautam, Optoelectron. Adv. Mater. – Rapid Comm. **1**(12), 655 (2007).
[31] R. S. Dubey, D. K. Gautam, Optoelectron. Adv. Mater. – Rapid Communic. **1**(9), 436 (2007).
[32] M. Popescu, D. Mezzane, Optoelectron. Adv. Mater. – Rapid Comm. **2**(1), 26 (2008).
[33] M. J. Ventura, C. Bullen, M. Gu, Optics Express **15**(4) 1817 (2007).
[34] M. Sima, I. Enculescu, M. Sima, Optoelectron. Adv. Mater. – Rapid Comm. **2**(2), 67 (2008).
[35] Johnson S. G., Joannopoulos J. D., Optics Express, 173, 2001.
[36] V. Dolghier, I. Vataman, A. Buzdugan, A. Popescu. Patent MD 967 C2/from 18.12.1997.

*Corresponding author: mpopescu@infim.ro